ECONSTOR
Make Your Publications Visible.

A Service of

ZBW Leibniz-Informationszentrum Wirtschaft
Leibniz Information Centre for Economics

Hänggi, Severin et al.

Article

A review of synthetic fuels for passenger vehicles

Energy Reports

Provided in Cooperation with:
Elsevier

Suggested Citation: Hänggi, Severin et al. (2019) : A review of synthetic fuels for passenger vehicles, Energy Reports, ISSN 2352-4847, Elsevier, Amsterdam, Vol. 5, pp. 555-569, https://doi.org/10.1016/j.egyr.2019.04.007

This Version is available at:
https://hdl.handle.net/10419/243610

Standard-Nutzungsbedingungen:

Die Dokumente auf EconStor dürfen zu eigenen wissenschaftlichen Zwecken und zum Privatgebrauch gespeichert und kopiert werden.

Sie dürfen die Dokumente nicht für öffentliche oder kommerzielle Zwecke vervielfältigen, öffentlich ausstellen, öffentlich zugänglich machen, vertreiben oder anderweitig nutzen.

Sofern die Verfasser die Dokumente unter Open-Content-Lizenzen (insbesondere CC-Lizenzen) zur Verfügung gestellt haben sollten, gelten abweichend von diesen Nutzungsbedingungen die in der dort genannten Lizenz gewährten Nutzungsrechte.

Terms of use:

Documents in EconStor may be saved and copied for your personal and scholarly purposes.

You are not to copy documents for public or commercial purposes, to exhibit the documents publicly, to make them publicly available on the internet, or to distribute or otherwise use the documents in public.

If the documents have been made available under an Open Content Licence (especially Creative Commons Licences), you may exercise further usage rights as specified in the indicated licence.


https://creativecommons.org/licenses/by-nc-nd/4.0/

WWW.ECONSTOR.EU

Mitglied der Leibniz-Gemeinschaft

Energy Reports 5 (2019) 555–569

Contents lists available at ScienceDirect

Energy Reports

journal homepage: www.elsevier.com/locate/egyr

Review article

A review of synthetic fuels for passenger vehicles

Severin Hänggi [a,*], Philipp Elbert [a], Thomas Bütler [b], Urs Cabalzar [b], Sinan Teske [b], Christian Bach [b], Christopher Onder [a]

[a] Institute for Dynamic Systems and Control, ETH Zurich, Sonneggstrasse 3, 8092 Zurich, Switzerland
[b] Department of Automotive Powertrain Technologies, Empa Dübendorf, Überlandstrasse 129, 8600 Dübendorf, Switzerland

ARTICLE INFO

Article history:
Received 13 August 2018
Received in revised form 11 March 2019
Accepted 16 April 2019
Available online xxxx

Keywords:
Power-to-gas
Power-to-liquid
Synthetic fuels
Renewable fuels
Well-to-wheels
Well-to-miles

ABSTRACT

Synthetic fuels produced with renewable surplus electricity depict an interesting solution for the decarbonization of mobility and transportation applications which are not suited for electrification. With the objective to compare various synthetic fuels, an analysis of all the energy conversion steps is conducted from the electricity source, i.e., wind-, solar-, or hydro-power, to the final application, i.e., a vehicle driving a certain number of miles. The investigated fuels are hydrogen, methane, methanol, dimethyl ether and Diesel. While their production process is analyzed based on literature, the usage of these fuels is analyzed based on chassis dynanometer measurement data of various EURO-6b passenger vehicles.

Conventional and hybrid power-trains as well as various carbon dioxide sources are investigated in two scenarios. The first reference scenario considers market-ready technology only, while the second future scenario considers technology which is currently being developed in industry and assumed to be market-ready in near future. With the results derived in this study and with consideration of boundary conditions, i.e., availability of infrastructure, storage technology of gaseous fuels, energy density requirements, etc., the most energy efficient of the corresponding suitable synthetic fuels can be chosen.

© 2019 The Authors. Published by Elsevier Ltd. This is an open access article under the CC BY-NC-ND license (http://creativecommons.org/licenses/by-nc-nd/4.0/).

Contents

* Corresponding author.
E-mail address: shaenggi@idsc.mavt.ethz.ch (S. Hänggi).

https://doi.org/10.1016/j.egyr.2019.04.007
2352-4847/© 2019 The Authors. Published by Elsevier Ltd. This is an open access article under the CC BY-NC-ND license (http://creativecommons.org/licenses/by-nc-nd/4.0/).

1. Introduction

1.1. Motivation

Modern society relies on a high degree of individual mobility and efficient transportation of goods. However, these sectors are responsible for a significant part of the global carbon dioxide emissions and are therefore contributing to global warming and climate change (Creutzig et al., 2015). Consequently, many countries promote the production of energy using renewable resources, such as wind-, solar- and hydro-power, and the corresponding technologies are mature and applied on a large scale (Reiche and Bechberger, 2004). The electrification of passenger and transportation vehicles promises a more sustainable and clean mobility and transportation, however, for some applications batteries may be unsuitable due to one or more of several effects: gravimetric energy density may be too low if the vehicle needs to be very lightweight, achieve a high degree of autonomy, or needs to exhibit a very short refueling time (Guzzella and Sciarretta, 2013). Typical examples of these types of applications are ships, long-haul trucks, but also some types of passenger vehicles.

As wind and solar irradiation cannot be controlled, the electricity production is expected to fluctuate more if a large number of renewable power plants are installed (Weitemeyer et al., 2015). Therefore, researchers have proposed to use excess electric energy produced by renewable power plants during periods of low demand to produce synthetic fuels, such as hydrogen, methane, methanol, dimethyl ether or synthetic Diesel (Luo et al., 2015). Conventional or hybrid-electric vehicles could then use these renewable synthetic fuels as an alternative to fossil fuels, in order to achieve a higher level of sustainability. The life-cycle of a synthetic fuel is typically divided into five steps:

1. Electrolysis of water to produce hydrogen.
2. Separation of carbon dioxide from the atmosphere or other sources.
3. Chemical synthesis and purification of the desired fuel.
4. Transportation and storage
5. Oxidation of the fuel in a fuel cell or combustion engine with release of gaseous water and carbon dioxide to the atmosphere.

This study presents an energy analysis of the whole life-cycle of the synthetic fuels hydrogen, methane, methanol, dimethyl ether and Diesel. For these fuels, the production process including carbon dioxide separation, storage and distribution is based on literature values. Section 3 describes the production of hydrogen for the generation of synthesis gas[1] or for the direct use as a fuel. In Section 4 various carbon dioxide capturing sources are described and evaluated and Sections 5–8 describe the processes that convert synthesis gas into the corresponding renewable fuel and state energy consumption values for production, storage and distribution.

In Section 2, the energy consumption of each vehicle type is derived. The approach applied here is based on drive cycle simulations based on vehicle models, which are developed and identified with own measurement data.

Section 9 compares the synthetic fuels and Section 10 presents a conclusion.

1.2. Research contribution

Synthetic fuels, their production and use in vehicles are well known in literature. However, the study presented here differs from literature in various aspects.

A large variety of energy consumption and efficiency values for all the conversion steps of the synthetic fuel production can be found in literature (Brynolf et al., 2018). Within the study presented here, energy consumption values are carefully chosen in order to represent todays market-ready technology and to predict its near-future development. Whenever possible, efficiency or energy consumption values are taken from commercially available technology or published data of test-plants. In addition, the authors own research and test plant data contributes to the accuracy of this study.

Existing comparisons of renewable fuels often place emphasis on production costs (Fasihi et al., 2016). The study presented here follows a systematic approach with the aim to compare different technologies and their influence on the overall energy consumption. Knowledge of the energy reduction potential and the development status of a technology allows the prediction of a near-future scenario.

While the majority of publications focuses on a Well-to-Wheels (WtW) analysis (Larsson et al., 2015), here a Well-to-Miles (WtM) comparison is conducted. Instead of a vehicle efficiency, the energy consumption of a vehicle driving a pre-defined

[1] The initial gas feed to the synthesis reactor consisting of either hydrogen and carbon dioxide or hydrogen and carbon monoxide is referred to as synthesis gas.

Table 1
Discussed fuels with their properties at standard conditions and their storage and tank pressure.

		Molar mass [g/mol]	H_l [kJ/mol]	H_u [kJ/mol]	p_{store} [bar]	p_{tank} [bar]
hydrogen	H_2	2.016	242	286	900	700
methane	CH_4	16.04	802	890	270	200
methanol	CH_3OH	32.04	638	727	1	1
DME	CH_3OCH_3	46.06	1321	1460	15	15
Diesel		∼170.0	∼7225	∼7720	1	1

speed profile is derived in simulation. This approach allows to include further technical characteristics such as power-train dependent vehicle mass differences or hybridization. For the drive cycle simulations, a vehicle model is introduced and identified with chassis dynanometer measurement data of various EURO-6b vehicles for each type of vehicle. This approach allows to accurately characterize and compare current power-train technologies. Further the model allows extrapolation to technologies which are technically realizable but not in series production, such as the natural gas hybrid vehicle.

To the authors knowledge, the well-to-miles energy analysis approach presented here is novel in this context and unpublished so far.

1.3. Preliminary information

Since the energy used to evaporate the water in the fuel production cannot be regained in an IC engine or in a fuel cell, this study states efficiency values for fuel production and usage referring to the lower heating value (H_l) of a particular fuel, as indicated in (1).

$$\eta_{prod} := \frac{H_l \cdot m_{fuel}}{E_{prod}} \qquad \eta_{use} := \frac{E_{wheels}}{H_l \cdot m_{fuel}} \tag{1}$$

Table 1 gives an overview of the fuel properties used for the calculations captured in this study. These values were taken from various sources, such as Semelsberger et al. (2006).

2. General approach for the tank-to-miles analysis

While the Well-to-Tank analysis for synthetic fuels is based on a literature review, the tank-to-wheels analysis is based on simulation results with underlying vehicle models, which are identified with chassis dynanometer measurement data.

The tank-to-miles analysis can be split up into the Wheels-to-Miles (WtM) and the Tank-to-Wheels (TtW) analysis.

2.1. Wheels-to-miles approach

Within the wheels-to-miles analysis, the mechanical power trajectory at the wheels $P_{wheels}(t)$ is determined for a given vehicle speed profile $v(t)$. The wheel power is dependent on vehicle specific characteristics, such as the rolling friction, the aerodynamic drag and the vehicle mass. Except for the mass, these parameters are independent of the vehicle specific propulsion system and its corresponding fuel.

The model approach stated in (2)–(5) is taken from Guzzella and Sciarretta (2013). It consists of a power balance. The wheel power P_{wheels} is equal to the power lost due to aerodynamic drag P_{aero} and rolling friction P_{roll}, and the power needed for the vehicle acceleration P_{acc}.

$$P_{aero}(t) = 0.5 \cdot \rho_{air} \cdot A_f \cdot c_d \cdot v^3(t) \qquad = 0.413 \cdot v^3(t) \tag{2}$$

$$P_{roll}(t) = m_{car} \cdot g \cdot c_r \cdot v(t) \qquad = 0.1275 \cdot m_{car} \cdot v(t) \tag{3}$$

$$P_{acc}(t) = m_{car} \cdot \frac{dv(t)}{dt} \cdot v(t) \tag{4}$$

$$P_{wheels}(t) = P_{aero}(t) + P_{roll}(t) + P_{acc}(t) \tag{5}$$

The gravitational acceleration $g = 9.81\ ^{m}/_{s^2}$ and the density of air at 25 °C $\rho_{air} = 1.18\ ^{kg}/_{m^3}$ are generally known. Values for the aerodynamic drag $A_f \cdot c_d = 0.7\ m^3$ and the rolling friction $c_d = 0.0013$ are taken from Guzzella and Sciarretta (2013). The total vehicle mass m_{car} was set to 1450 kg for conventional simple propulsion systems, while for hybrid or fuel cell propulsion systems, a total mass of 1650 kg was used. For electric vehicles the mass was set to 1750 kg to account for the increased battery mass.

As a speed profile, the worldwide harmonized light vehicles class 3 test cycle (WLTC class 3) is chosen. With this cycle and (2)–(6), the wheel power trajectory and the mean energy demand per kilometer $E_{wheels,norm}$ can be determined. The latter can also be seen as the energy consumption of a vehicle with 100% fuel-to-traction efficiency and 100% recuperation efficiency, as described in Ott et al. (2013).

$$E_{wheels,norm} = \frac{\int P_{wheels}(t)dt}{\int v(t)dt} \tag{6}$$

For the conventional passenger car with a mass of 1450 kg, the mean energy demand at the wheels is equal to 0.41 MJ/km and for the car with a hybrid or fuel cell propulsion system, the mean energy takes a value of 0.44 MJ/km. The electric vehicle has a mechanical energy demand of 0.45 MJ/km.

2.2. Tank-to-wheels analysis

The tank-to-miles analysis considers the conversion of the chemical power in the tank to mechanical power at the vehicle wheels. It is strongly dependent on its underlying propulsion system and the fuel characteristics.

The equations used to model the different propulsion systems are stated in (7). They directly connect the wheel power P_{wheels} with the chemical power P_{chem} stored in the vehicles tank. This static model is based on a Willans approach, similar to the evaluations in Bach and Soltic (2011), but extended to negative wheel power in order to account for the possibility of recuperation for electrified power-trains. For vehicles unable to recuperate energy, the parameter $c_{1,neg}$ is set to zero.

$$P_{chem}(t) = \begin{cases} c_{1,pos} \cdot P_{wheels}(t) + c_{0,pos}, & P_{wheels}(t) \geq 0 \\ c_{1,neg} \cdot P_{wheels}(t) + c_{0,neg}, & P_{wheels}(t) < 0 \end{cases} \tag{7}$$

In order to identify the propulsion system model parameters ($c_{1,pos}$, $c_{0,pos}$, $c_{1,neg}$ $c_{0,neg}$) for each type of fuel, chassis dynanometer measurements of various EURO-6b passenger car types are evaluated. Table 2 gives an overview of the conducted measurement series and states the mean identified model parameters dependent on the power-train technology. As an indicator for the model accuracy, R^2 states the mean coefficient of determination.

The 18 EURO6b vehicles which were used to identify these parameters are listed in Table 3. Fig. 1 illustrates the results stated in Table 2 with the corresponding tank-to-wheels efficiency η_{TtW} as defined in (8).

$$\eta_{TtW}(t) = \begin{cases} \frac{P_{wheel}(t)}{P_{chem}(t)}, & P_{wheel}(t) \geq 0 \\ \max\left(0, \frac{P_{chem}(t)}{P_{wheel}(t)}\right), & P_{wheel}(t) < 0 \end{cases} \tag{8}$$

For electric and fuel cell vehicles, the corresponding identified models are directly used for the tank-to-wheels analysis. For propulsion systems operated with other fuels, the model parameters are derived by adapting the available models accordingly. The following assumptions are used to derive these models:

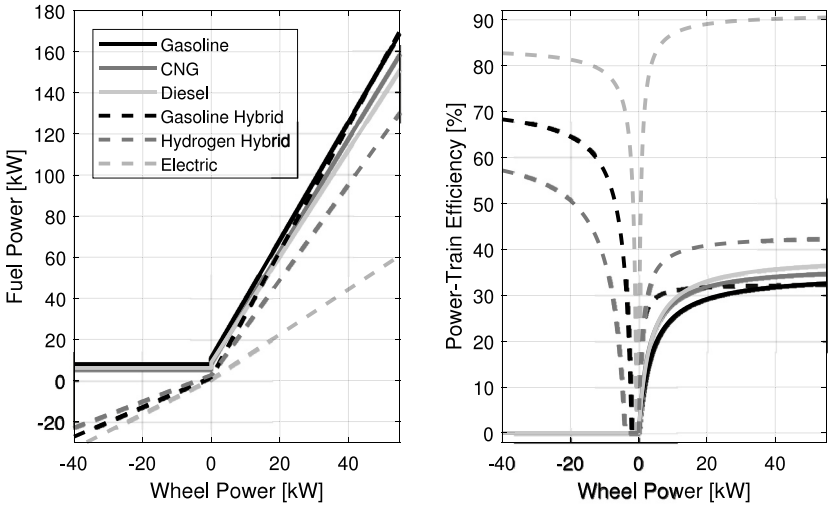

Fig. 1. Illustration of the identified tank-to-wheel models stated in Table 2.

Table 2
Tank-to-wheel mean model parameters including their standard deviation σ for different types of EURO-6b power-train technologies, identified with chassis dynanometer measurement data (WLTC class 3 test cycle)..

No. of vehicles		Gasoline	Gasoline hybrid	CNG	Diesel	Hydrogen hybrid	Electric
		6	2	1	6	1	2
$c_{1,\text{pos}}$	[−]	2.87	3.07	2.73	2.58	2.32	1.09
$\sigma_{c_{1,\text{pos}}}$	[−]	0.084	0.082	0	0.27	0	0.028
$c_{0,\text{pos}}$	[kW]	11.16	1.52	8.14	8.83	2.63	0.56
$\sigma_{c_{0,\text{pos}}}$	[kW]	3.19	2.33	0	1.17	0	0.09
$c_{1,\text{neg}}$	[−]	0	0.72	0	0	0.64	0.84
$\sigma_{c_{1,\text{neg}}}$	[−]	0	0.014	0	0	0	0.078
$c_{0,\text{neg}}$	[kW]	7.94	1.52	5.44	6.10	2.63	0.56
$\sigma_{c_{0,\text{neg}}}$	[kW]	1.24	2.33	0	1.09	0	0.09
R^2	[%]	96.8	91.4	97.7	92.0	91.7	99.2
σ_{R^2}	[%]	0.5	0.6	0	2.0	0	0.5

Table 3
EURO 6b vehicles used to identify the model parameters stated in Table 2.

Gasoline	Suzuki SX4-Cross Fiat 500 BMW 428i	Skoda Octavia C 1.8 4 × 4 Alfa-Romeo Giulietta 1.4 TB VW Golf VII R
Gasoline hybrid	VW Jetta Hybrid	Audi A3 Sportback e-tron
CNG	Audi A3 Sportback g-tron	
Diesel	Mini Cooper D Opel Astra K 16DTH ST BMW X3 xDrive 20D	Ford S-Max 2.0 TDCi Peugeot 308 SW Blue HDI Mercedes-Benz A220 CDI
Hydrogen hybrid	Hyundai ix35	
Electric	VW e-Golf	Ford Focus Electric

- Methanol and methane vehicles perform equally to the identified CNG vehicle.
- Fischer–Tropsch (FT) Diesel and DME power-trains perform equally to the model identified with six Diesel vehicles (Verbeek and Van der Weide, 1997).
- Methane, methanol, DME and Diesel hybrid vehicles have the same recuperation efficiency.
- At a positive wheel power of 50 kW, hybrid vehicles have the same efficiency as their conventional equivalent. This assumption holds for hybrid vehicles operated in a charge-sustaining mode, where the electric unit is used to increase part-load efficiency while for high loads the combustion engine delivers the complete power. In Fig. 1, this behavior can be observed by comparing the gasoline hybrid model with the conventional gasoline model.

Table 4
Tank-to-wheel model parameters for the vehicle types covered within this study, adapted from Table 2.

Power-train	$c_{1,\text{pos}}$	$c_{0,\text{pos}}$	$c_{1,\text{neg}}$	$c_{0,\text{neg}}$
Methanol	2.73	8.14	0	5.44
Methanol Hyb.	2.87	1.52	0.72	1.52
Methane	2.73	8.14	0	5.44
Methane Hyb.	2.87	1.52	0.72	1.52
DME	2.58	8.83	0	6.10
DME Hyb.	2.73	1.52	0.72	1.52
Diesel	2.58	8.83	0	6.10
Diesel Hyb.	2.73	1.52	0.72	1.52
Hydrogen	2.32	2.63	0.64	2.63
Electric	1.09	0.56	0.84	0.56

The application of these assumptions leads to the complete set of propulsion system model parameters for each fuel considered in this study. Table 4 states the corresponding values and Fig. 2 illustrates these propulsion models.

In order to derive the fuel individual tank-to-wheels efficiency, the propulsion system models stated in (7) are applied to the corresponding wheel power profile derived in Section 2.1. The results are presented in Table 5. Conventional propulsion systems have a tank-to-wheels efficiency η_{TtW} between 21% and 22%. Hybridization (operated in charge-sustaining mode) can increase the efficiency up to 6%. A fuel cell propulsion system allows a further increase to 30.9%.

For the electric vehicle, two simulation results are derived. While the first simulation consists of a tank-to-miles analysis, the second simulation additionally considers battery charging losses. For the two electric cars mentioned in Table 2, a mean charging efficiency of 76% was identified with measurement data.

The derived energy consumption values stated in Table 5 will be used within the further well-to-miles analysis.

3. Hydrogen

Water electrolysis represents an efficient large-scale method to produce renewable hydrogen. It splits liquid water into hydrogen and oxygen, which corresponds to the reverse reaction of the hydrogen combustion. Therefore, its enthalpy ΔH_R is equal to the upper heating value of hydrogen. As shown in (10), the enthalpy is equal the sum of the Gibbs free energy ΔG_R and the

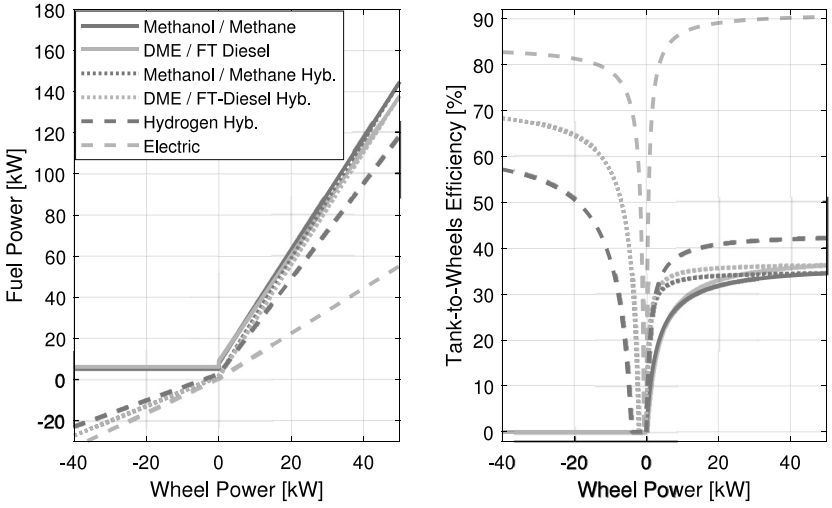

Fig. 2. Illustration of the tank-to-wheel models stated in Table 4.

Table 5
WLTC class 3 test cycle simulation results for all investigated vehicle types.

	m_{car} [kg]	$E_{chem,norm}$ [MJ/km]	$\eta_{TtW,mean}$ [%]
Methanol	1450	1.94	21.2
Methanol Hyb.	1650	1.65	26.6
Methane	1450	1.94	21.2
Methane Hyb.	1650	1.65	26.6
DME	1450	1.91	21.6
DME Hyb.	1650	1.57	28.0
Diesel	1450	1.91	21.6
Diesel Hyb.	1650	1.57	28.0
Hydrogen	1650	1.42	30.9
Electric	1750	0.57	79.5
Electric recharged		0.75	59.8

entropy $T\Delta S_R$. While the Gibbs free energy has to be delivered by electricity, the entropy can be delivered by either a thermal or an electric energy source (Töpler and Lehmann, 2014).

$$H_2O(l) \longrightarrow H_2 + {}^1/_2O_2 \quad \Delta H_R = +286\ {}^{kJ}/_{mol} \tag{9}$$

$$\Delta H_R = \Delta G_R + T\Delta S_R \tag{10}$$

Using the definition stated in (1), the maximum theoretical efficiency of the hydrogen production is given by the ratio of H_l and H_u and corresponds to 85%.

3.1. Production process

According to Töpler and Lehmann (2014), there exist three main electrolysis methods, distinguished by their electrolyte:

- Alkaline water electrolysis, working with a liquid alkaline electrolyte solution (normally consisting of about 30% of potassium hydroxide).
- Proton Exchange Membrane (PEM) electrolysis with a solid polymer electrolyte.
- High-temperature electrolysis with a solid oxide electrolyte cell (SOEC).

The alkaline electrolysis usually uses liquid water at a temperature around 80 °C and a pressure between 1–60 bar. It is the most common water electrolysis method nowadays and it is used in industry for large-scale hydrogen production. Eqs. (11) and (12) state the chemical reactions on the cathode and anode side of the electrolysis cell (Töpler and Lehmann, 2014). The two sides are separated by a diaphragm that prevents the mixing of O_2 and H_2 but is permeable for OH^-, which is transported from the cathode to the anode side. Potassium hydroxide acts as an electrolyte and increases the water conductivity. Recent improvements in this method allow dynamic electrolysis operation within a load range between 10% and 110% of the nominal power and a load change rate of approximately 15 %/s (ETOGAS GmbH, 2015).

$$\text{Cathode}: \quad 2H_2O + 2e^- \longrightarrow H_2 + 2OH^- \tag{11}$$

$$\text{Anode}: \quad 2OH^- \longrightarrow {}^1/_2O_2 + H_2O + 2e^- \tag{12}$$

The development of the PEM electrolysis started in the 1990s. So far, only a few small-scale test plants have been built. Eqs. (13) and (14) denote the chemical reactions on the anode and cathode side, which are separated by a proton exchange membrane (permeable for H^+). The water enters the cell on the anode side, where it is split into two H^+ ions, oxygen and two electrons. While the electrons are adsorbed by the anode, the electric field between the anode and the cathode causes the ions to move from the anode side through the membrane to the cathode side. There they react with two electrons to hydrogen (Töpler and Lehmann, 2014).

$$\text{Anode:} \quad H_2O \longrightarrow 2H^+ + {}^1/_2O_2 + 2e^- \tag{13}$$

$$\text{Cathode:} \quad 2H^+ + 2e^- \longrightarrow H_2 \tag{14}$$

This electrolysis process works with similar pressure and temperature as the alkaline electrolysis, but it reaches a higher current density and can be operated much more dynamically. Load changes between 0% and 100% can be completed within fractions of a second, which is one of the main advantages of this technology.

The high-temperature electrolysis works in a temperature range between 700–900 °C and is the only technology that uses thermal as well as electric energy for water splitting. The use of waste heat from another process allows for a high overall energy efficiency. At a temperature of 800 °C, approximately 100 ${}^{kJ}/_{mol\ H_2}$ or one third of total energy can be provided by thermal energy (Ursua et al., 2012). As shown in (15) and (16), the reactions on the cathode and anode side are similar to the reactions of the alkaline method, but instead of OH^-, O^{2-} is transferred from the cathode through a solid-oxide electrolyte to the anode.

$$\text{Cathode:} \quad H_2O + 2e^- \longrightarrow H_2 + O^{2-} \tag{15}$$

$$\text{Anode:} \quad O^{2-} \longrightarrow {}^1/_2O_2 + 2e^- \tag{16}$$

While a few years ago the high temperature electrolysis cell was assumed to operate in steady-state conditions only

Table 6
State of the art efficiency and capacity characterization of different electrolysis methods, taken from Gallandat et al. (2017) and Sunfire GmbH (2017).

	Capacity [^{N} m^3/h]	Efficiency [%]
Alkaline	1–500	53–62
PEM	4–225	51–62
High-Temperature	40	67 (82)

(Wendt and Vogel, 2014), recent developments disproved these statements. Today there exist market-ready small-scale high-temperature electrolysis systems able to dynamically adapt their load (Sunfire GmbH, 2017).

In Table 6 the efficiency values of current industry systems for each type of electrolysis method are listed. These values refer to the whole hydrogen production unit including the thermal management, the purification of hydrogen and further auxiliaries. For alkaline and PEM systems, values were taken from Gallandat et al. (2017), while Sunfire GmbH (2017) was used for the high temperature electrolysis. The values were verified with the manufacturer, corrected if necessary and adapted to the lower heating value as a reference. For the high-temperature electrolysis, the value in brackets states the efficiency without consideration of the required thermal energy.

Due to the promotion of renewable energy, electrolysis and clean fuel production in general became a strongly researched topic. Besides the progress in performance, initial electrolysis costs are expected to be strongly reduced and large-scale PEM plants as well as large scale high-temperature electrolysis plants are expected to be market-ready within the next few years.

3.2. Compression

Compared to other fuels, hydrogen has a very low volumetric energy density. Fuel cell vehicles commonly use a tank pressure of either 350 bar or 700 bar, where only the higher tank pressure allows for a driving range comparable to a gasoline vehicle at an appropriate tank size. In order to fill a vehicle tank within few minutes, gas stations use storage tanks with a pressure p_1 of 900 bar. The energy needed for the compression depends on the pressure ratio as well as the temperature increase during the compression. The pressure ratio is given by the storage pressure and the initial hydrogen pressure p_0 after the electrolysis process or after transportation, which is set to 5 bar. Assuming an ideal isothermal process ((17), Bossel, 2006), the compression would need about 12.7 $^{kJ}/_{mol\ H_2}$. Assuming no heat transfer at all, the compression can be described as an ideal adiabatic process ((18), Bossel, 2006) and would consume about 29.7 $^{kJ}/_{mol\ H_2}$. Real compressors operate between these two limits and try to get close to the isothermal limit by using several compression stages with cooling in between. Linde recently developed an ionic compressor consuming about 19.6 $^{kJ}/_{mol\ H_2}$ (The Linde Group, 2017) for the compression of hydrogen from 5 bar to 900 bar, which corresponds to about 8.1% of the lower heating value of hydrogen.

$$E_{isoth} = p_0 V_0 \log\left(\frac{p_1}{p_0}\right) \tag{17}$$

$$E_{adi} = p_0 V_0 \frac{\gamma}{\gamma - 1}\left(\left(\frac{p_1}{p_0}\right)^{\frac{\gamma-1}{\gamma}} - 1\right) \tag{18}$$

3.3. Transportation

The transportation of hydrogen can be realized by pipeline or by road transportation. For road transportation, The Linde Group (2013) presents a tube trailer, able to carry 1100 kg of hydrogen at 500 bar. At the fuel station, the truck releases hydrogen into a buffer vessel until buffer and trailer tubes reach a common pressure of 50 bar (about 140 kg of H_2 remains in the trailer tubes). Assuming a fuel cell hybrid trailer with the efficiency stated in Table 5, the H_2 transportation consumes 1.5 $^{\%}/_{100\ km}$ of the transported hydrogen. The energy needed for the compression of hydrogen from 5 bar to 500 bar into the trailer tubes is calculated by (19) and consumes about 17.5 $^{kJ}/_{mol\ H_2}$, which corresponds to 7.2% of its lower heating value. Hydrogen pipelines offer a huge decrease in energy consumption since the transportation could take place with far lower pressure. An electric energy consumption of 0.77 $^{\%}/_{100\ km}$ is stated in Bossel (2006), which corresponds to approximately 2 $^{kJ}/_{mol\ H_2}$. However, currently such infrastructure is not available.

Table 7
Hydrogen well-to-tank analysis for a reference and a near future scenario.

	Reference scenario	Future scenario
Electrolysis	PEM/Alkaline 403 $^{kJ}/_{mol\ H_2}$ 60%	SOEC 361 $^{kJ}/_{mol\ H_2}$ 67%
Storage, Transportation & Cooling	900 bar/tube trailer 46.0 $^{kJ}/_{mol\ H_2}$ elec. 98.5% (transportation)	900 bar/pipeline 29.8 $^{kJ}/_{mol\ H_2}$ elec. 100%
Well-to-tank Efficiency	53%	62%
Well-to-miles FC hybrid car	16.5% 2.7 $^{MJ}/_{km}$	19.1% 2.3 $^{MJ}/_{km}$

$$E_{comp} = \frac{1}{2}(E_{adi} + E_{isoth}) \tag{19}$$

3.4. Fueling process

Hydrogen fuel stations need to cool hydrogen to -40 °C in order to prevent the hydrogen vessels from overheating during the refueling process. Considering the heat capacity of hydrogen, about 1.7 $^{kJ}/_{mol\ H_2}$ of thermal energy has to be removed by a cooling device. A measurement series in a prototype hydrogen filling station in Switzerland (Cabalzar and Stadelmann, 2017) showed that this cooling process consumes about 3% of the energy stored in hydrogen.

3.5. Well-to-miles analysis

A reference and a future scenario are considered. While the reference scenario is based on mature technology, the future scenario describes a best-case estimation with new technology, which is not available for large-scale production yet, and infrastructure which is not given yet. A well-to-tank analysis of these scenarios is presented in Table 7.

The reference scenario describes a centralized large-scale hydrogen production plant based on PEM or alkaline electrolysis, which is 150 km away from the hydrogen fuel station. The transportation with a tube trailer as well as the compression into storage vessels and the cooling during the refilling process are considered within the analysis. The future scenario is similar to the reference, but with a more efficient SOEC electrolysis system and pipeline transportation instead of road transportation.

Considering a decentralized small-scale plant directly integrated into a filling station, the transportation with its compression can be neglected. Storage and refilling would consume 26.8 $^{kJ}/_{mol\ H_2}$ or 11.1% instead of 46 $^{kJ}/_{mol\ H_2}$ or 20.5% of the hydrogen energy content, as it is the case for a centralized plant (with road transportation). However, due to a higher auxiliary power ratio

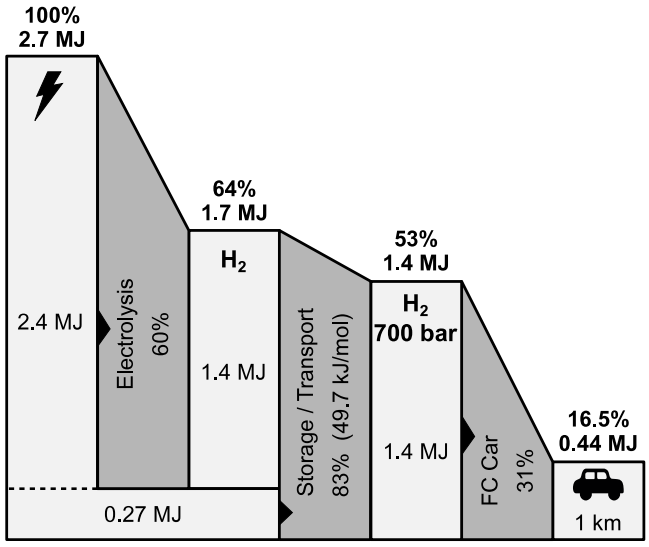

Fig. 3. Well-to-miles reference scenario for hydrogen, used in a fuel cell vehicle, with consideration of storage and transportation losses.

the efficiency of a small-scale electrolysis plant is expected to be lower compared to a centralized large-scale plant.

For the reference scenario, the well-to-miles analysis is illustrated in Fig. 3. In order to drive one kilometer with a fuel cell hybrid vehicle, 0.44 MJ of mechanical energy at the vehicle wheels and 1.4 MJ of chemical energy in the tank are needed as derived in Section 2. Storage and transportation of the hydrogen need 0.27 MJ or 10% of the initial electric energy, and the hydrogen production by electrolysis consumes 2.4 MJ for a 1 km drive. Energy losses mainly occur in the fuel cell power-train and during the hydrogen production.

4. CO_2 separation

Except for hydrogen, all synthetic fuels considered in this study are carbon-based and produced by synthesis gas consisting of hydrogen and either carbon dioxide (CO_2) or carbon monoxide (CO), obtained by the reduction of carbon dioxide. This reduction as well as the capture of CO_2 is covered in this section.

$$H_2O(l) \longrightarrow H_2 + {}^1/_2O_2 \quad + 286\ {}^{kJ}/_{mol} \tag{20}$$

$$H_2 + CO_2 \longleftrightarrow CO + H_2O(g) \quad + 41\ {}^{kJ}/_{mol} \tag{21}$$

Eq. (21) states the reverse water-gas shift reaction, which represents the most common way to reduce CO_2 to CO. Depending on the fuel, this process is carried out in a separate reactor before the fuel synthesis, or it is integrated in the fuel synthesis itself to be able to feed the system with CO_2 directly. For the production of one mole CO, one mole of hydrogen is needed, which results in a total reaction enthalpy of 327 ${}^{kJ}/_{mol}$.

An alternative method is offered by the high-temperature electrolysis process, which is able to simultaneously reduce H_2O and CO_2 (co-electrolysis) and therefore directly produces a H_2-CO mixture ready for synthetic fuel production (Fu et al., 2010). Eq. (22) states the reduction of CO_2 as it takes place in the co-electrolysis process. Since there is no water evaporated in this reaction, its enthalpy is 13.5% lower compared to the reverse water-gas shift reaction process.

$$CO_2 \longleftrightarrow CO + {}^1/_2O_2 \quad + 283\ {}^{kJ}/_{mol} \tag{22}$$

Carbon dioxide has to be extracted out of air, water or biomass. A further option is to capture the carbon dioxide out of flue gas (from renewable power generation, such as biogas power plants). Except for the CO_2 extraction out of seawater, all capturing methods are based on amine adsorption, a cyclic process mainly using thermal energy.

4.1. The atmosphere as a carbon source

The concentration of CO_2 in the air is approximately 0.04% (56 m^3 of air contain one mole of CO_2), which is why a large volume has to be processed for the carbon dioxide separation. Therefore, a large amount of energy is required for this method. The two literature sources Zeman (2007) and Gebald (2014) both state an energy consumption of 350 ${}^{kJ}/_{mol\ CO_2}$. An existing test plant, built by Climeworks (Evans, 2017), consumes 400 ${}^{kJ}/_{mol\ CO_2}$ of thermal- and 80 ${}^{kJ}/_{mol\ CO_2}$ of electric energy.

4.2. Seawater as a carbon source

The carbon concentration in the air is in balance with the carbon concentration in seawater. Therefore, CO_2 can be separated out of sea water in order to lower the concentration in the atmosphere. The advantage of this process is that the volumetric CO_2 concentration in seawater is about 140 times higher than in the air (Willauer et al., 2014). A process that needs 242 ${}^{kJ}/_{mol\ CO_2}$ is presented in Eisaman et al. (2012).

4.3. Flue gas as a carbon source

The separation of CO_2 from flue gas requires less energy since its concentration is approximately 250 times higher than in air. A selection of methods with the appropriate thermal and electric energy consumption is listed in Desideri and Paolucci (1999). The required thermal energy takes values of 160–250 ${}^{kJ}/_{mol\ CO_2}$ and the electric energy consumption lies between 2–20 ${}^{kJ}/_{mol\ CO_2}$.

The thermal energy could be delivered by the waste heat of the power plant itself or it could be the waste heat of a chemical reaction, such as the synthesis of a renewable fuel. Such a symbiosis is covered in Reiter and Lindorfer (2015), where the separation of CO_2 from flue gas uses waste heat from the methane synthesis process. Apart from 163 ${}^{kJ}/_{mol\ CO_2}$ of thermal energy, 10 ${}^{kJ}/_{mol\ CO_2}$ of electric energy needs to be supplied to the separation process.

4.4. Biomass as a carbon source

Biogas plants produce a gas mixture of methane and carbon dioxide. If it is used as natural gas, CO_2 needs to be separated and is therefore a side product of the bio methane production. The CO_2 concentration in biogas can reach high values of 25% to 55% and the CO_2 separation process has a total energy consumption of approximately 90 ${}^{kJ}/_{mol\ CO_2}$ (Müller et al., 2011). For further analysis, we assume that similar to flue gas the majority of 80 ${}^{kJ}/_{mol\ CO_2}$ can be supplied as thermal energy.

5. Methane

Methane is the main component of natural gas, one of the most common fossil fuels. It is mainly extracted from natural gas fields or produced from shale or coal.

Renewable methane can either be produced in biogas plants by fermentation or anaerobic digestion, or it can be produced by the synthesis of hydrogen and carbon dioxide (Sabatier process). The following sections concentrate on the renewable CH_4 production by synthesis gas.

Eq. (25) states the Sabatier reaction as it is given in Müller et al. (2011). It consists of two reaction steps. First, carbon monoxide is produced by the reverse water-gas shift reaction stated in (23) and afterwards the methanation step given in (24) converts hydrogen and carbon monoxide to methane and water.

$$H_2 + CO_2 \longleftrightarrow CO + H_2O \quad + 41\ ^{kJ}/_{mol} \tag{23}$$

$$3H_2 + CO \longleftrightarrow CH_4 + H_2O \quad - 206\ ^{kJ}/_{mol} \tag{24}$$

In total, one mole of methane is produced out of four moles of hydrogen. A comparison of the lower heating values shows that only 83% of the energy in hydrogen is stored in methane after the conversion. Since the overall reaction is an exothermic process, no additional energy source is needed and the stated value can be considered to be the theoretical maximum efficiency of the hydrogen conversion to methane.

$$CO_2 + 4H_2 \longleftrightarrow CH_4 + 2H_2O \quad - 165\ ^{kJ}/_{mol} \tag{25}$$

The total methane production process consists of the hydrogen production and the methanation. The theoretical maximum efficiency for the whole synthetic methane production process can be calculated by multiplying the theoretical maximum efficiency values of both process steps, which leads to a value of 70%. If the reaction heat of the Sabatier process ($-165\ ^{kJ}/_{mol\ CH_4}$) is used to provide a major part of the required entropy ($176\ ^{kJ}/_{mol\ CH_4}$) for the high-temperature electrolysis, the theoretical maximum efficiency of the overall process increases to 82%. A further increase in the theoretical maximum efficiency is achieved by the co-electrolysis. If CO_2 is reduced to CO directly within the high-temperature electrolysis process, the maximum efficiency increases to 86%. However, all these theoretical calculations neglect the energy used for the CO_2 separation.

5.1. Synthesis

As shown in (25), the Sabatier process is an equilibrium reaction. It takes place in a reactor at a pressure of 6–7 bar and a temperature of 180–350 °C (Reiter and Lindorfer, 2015). A catalyst accelerates the reaction towards the equilibrium which is desired to be as far on the product side of the reaction as possible. Different types of nickel catalysts used for the CO_2 methanation are listed in Aziz et al. (2015). They are compared by their selectivity, the conversion percentage and other qualities. Most of them have an excellent selectivity, which means that there are nearly no side reactions that lead to other products than methane and water. Therefore it is assumed that efficiency losses due to unwelcome side reactions are negligible.

The outcome of the Sabatier process contains water, methane and depending on the conversion rate hydrogen and CO/CO_2. Normally the conversion rate is high enough to directly feed the product gas into the natural gas grid and to use it as a fuel after a drying process. However, if the reactor is not at its operation temperature during the warm-up phase, the Sabatier process product gas needs to be recirculated into the reactor. Since the catalytic reaction is an exothermic process operated at low pressure, the energy consumption of the synthesis process is assumed to be small and its efficiency is set to 80% ($34.5\ ^{kJ}/_{mol\ CH_4}$), which is close to the theoretical maximum value.

5.2. Storage and transportation

Compared to hydrogen, methane can be stored and transported in the existing natural gas grid. Pipelines need about 1% of the energy stored in methane for the transportation of about 450 km (Bossel, 2006).

Due to a higher volumetric energy density, methane fueled cars have a tank pressure of 200 bar which is considerably lower than the tank pressure of fuel cell vehicles. To provide fast refueling, gas stations store methane in a buffer vessel at 270 bar. As it is the case for hydrogen, the energy needed to compress methane with a multi-stage compressor lies in between the isothermal and adiabatic limit (Bossel, 2006). In order to calculate the energy for a compression from atmospheric pressure into the buffer vessel, (17)–(19) are used with methane specific parameters. The calculation results in a consumption of $17\ ^{kJ}/_{mol\ CH_4}$ or 2.1% of the energy stored in methane, related to its lower heating value.

Considering the compression energy and a pipeline transport of 150 km, the total storage and transportation energy consumption amounts to $19.7\ ^{kJ}/_{mol\ CH_4}$.

Table 8
Synthetic methane well-to-miles analysis for a reference and a near future scenario, depending on the source of carbon dioxide [biogas, flue gas, seawater, air].

	Reference scenario	Future scenario
Electrolysis	PEM/Alkaline $1612\ ^{kJ}/_{mol\ CH_4}$ 60%	SOEC co-electrolysis $1256\ ^{kJ}/_{mol\ CH_4}$ 80%
CO_2 Separation	for biogas , flue gas, seawater and air: $[90, 175, 242, 350]\ ^{kJ}/_{mol\ CH_4}$	
CH_4 Synthesis	Heat unused $34.5\ ^{kJ}/_{mol\ CH_4}$	Heat → SOEC $34.5\ ^{kJ}/_{mol\ CH_4}$
Storage & Transportation	270 bar/150 km pipeline $19.7\ ^{kJ}/_{mol\ CH_4}$	
Well-to-tank Efficiency	[46, 44, 42, 40]%	[57, 54, 52, 48]%
Well-to-miles Hybrid car	[12.2, 11.6, 11.2, 10.6]% $[3.6, 3.8, 3.9, 4.2]\ ^{MJ}/_{km}$	[15.3, 14.4, 13.8, 12.9]% $[2.9, 3.1, 3.2, 3.4]\ ^{MJ}/_{km}$
Well-to-miles Conv. Car	[9.7, 9.2, 8.9, 8.4]% $[4.3, 4.5, 4.6, 4.9]\ ^{MJ}/_{km}$	[12.2, 11.5, 11.0, 10.3]% $[3.4, 3.6, 3.8, 4.0]\ ^{MJ}/_{km}$

5.3. Well-to-miles analysis

As for hydrogen, a reference and a future scenario are considered for the well-to-miles analysis and summarized in Table 8.

The reference scenario describes a large-scale synthetic methane production plant based on PEM or alkaline electrolysis, which is 150 km away from the filling station. The energy consumption of the CO_2 separation, the synthesis process, the transportation within the natural gas grid and the compression to 270 bar into storage vessels are considered within the analysis.

As a future scenario we consider a methane production setup with high-temperature electrolysis, in which the waste heat of the methanation is reused for the generation of high temperature steam. Also CO_2 is reduced to CO directly within the high-temperature electrolysis (co-electrolysis). The methanation process therefore consists of the reaction stated in (24) only and has a higher thermal energy output, of which 90% or $185\ ^{kJ}/_{mol\ CH_4}$ are reused. The high-temperature efficiency stated in Table 6 increases to 80%.[2]

For the reference scenario and biogas as a CO_2 source, the well-to-miles analysis is illustrated in Fig. 4. In order to drive one kilometer with a conventional CNG vehicle, 0.41 MJ of mechanical energy at the vehicle wheels and 1.9 MJ of chemical energy in the tank are needed as derived in Section 2. While CO_2 separation, methanation, storage and transportation need 0.35 MJ or 8% of the total electric energy, the electrolysis plant consumes 3.9 MJ for the hydrogen production.

[2] This value was calculated with the assumption that the reduction of CO_2 to CO is equally efficient, with respect to the higher heating value, as the reduction of H_2O to H_2.

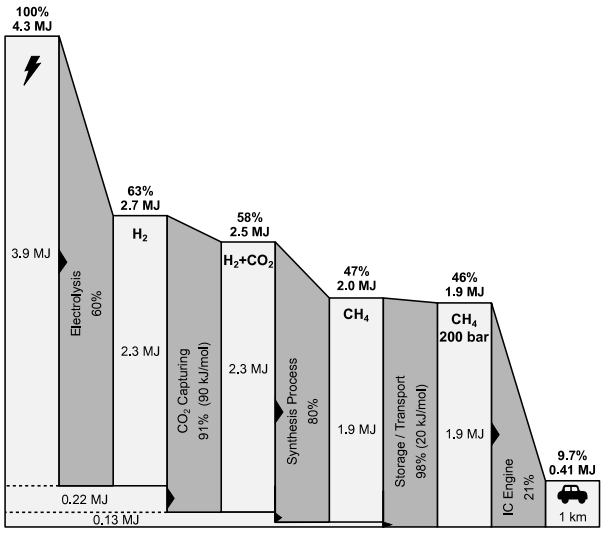

Fig. 4. Well-to-miles reference scenario for methane, used in a conventional IC engine vehicle. CO_2 is captured out of biogas.

Similar to the fuel cell vehicle, the propulsion system and the electrolysis process have the highest energy losses. Especially the conventional power-train has a very low mean efficiency. The introduction of a hybrid power-train would reduce the total electricity consumption by 16% from 4.3 MJ to 3.6 MJ. As shown in Table 8 for the future scenario, the reduction potential of the high-temperature co-electrolysis is especially high for the methane production. In addition to its higher efficiency and the possibility to integrate the CO_2 reduction, it allows to reuse thermal excess energy of the methanation process to further increase the overall efficiency. Compared to the reference scenario, the future scenario allows to further reduce the total energy input by approximately 20%.

The source of CO_2 has a significant influence on the well-to-miles analysis. Using the air as a carbon source would increase the overall energy consumption by 14% from 4.3 MJ to 4.9 MJ in the reference scenario with a conventional power-train.

6. Methanol

Similar to methane, methanol can be generated from synthesis gas in an exothermic reaction. It is liquid at standard conditions and can therefore be better stored and transported compared to hydrogen or methane.

Methanol can either be synthesized directly by hydrogen and carbon dioxide (26), or in two steps with the reverse water-gas shift reaction followed by the conversion of carbon monoxide and hydrogen to methanol (27) (Jadhav et al., 2014).

$$CO_2 + 3H_2 \longleftrightarrow CH_3OH + H_2O \qquad [-50]\ ^{kJ}/_{mol} \tag{26}$$

$$\begin{aligned} 2H_2 + CO &\longleftrightarrow CH_3OH \quad -91\ ^{kJ}/_{mol} \\ H_2 + CO_2 &\longleftrightarrow CO + H_2O \quad +41\ ^{kJ}/_{mol} \end{aligned} \tag{27}$$

Both reaction paths need three moles of hydrogen and one mole of carbon dioxide to produce one mole of methanol. About 88% of the energy stored in hydrogen can be found in methanol after the synthesis process. Both reaction paths are exothermic, which is why no additional thermal energy is required and the stated value can be seen as the theoretical maximum efficiency of the hydrogen-to-methanol conversion.

The theoretical maximum electricity-to-methanol efficiency is equal to 74%. If the synthesis heat is reused in a high-temperature electrolysis process, this value increases up to 79%. A further increase to 84% is achieved if CO_2 is reduced to CO by co-electrolysis. In these theoretical calculations, the energy used for the CO_2 separation is not included.

6.1. Synthesis

The conversion from synthesis gas to methanol takes place in a reactor with a pressure of 60-80 bar and temperature between 220-280 °C. The conversion rate of CO_2 is in the range of 35% to 45%. The unconverted synthesis gas is separated from the reaction products and reused. From the resulting products, methanol is separated from water and dissolved gases by distillation. As for the methane synthesis the catalysts have a very high selectivity. Side products are in the range of 400 ppm (Wernicke et al., 2014).

According to Van-Dal and Bouallou (2013), the total synthesis process from CO_2 and H_2 to methanol including the purification has an electric energy consumption of approximately 40 $^{kJ}/_{mol\ CH_3OH}$. Further losses occur due to purging processes, which contain a small fraction of the synthesis gas. The process described in Van-Dal and Bouallou (2013) uses approximately 3.24 $^{molH_2}/_{mol\ CH_3OH}$ instead of 3 $^{molH_2}/_{mol\ CH_3OH}$, which corresponds to a 7% energy loss during the synthesis process. For a further analysis, we assume that the purge gas is used in a burner to produce a thermal energy of 55 $^{kJ}/_{mol\ CH_3OH}$, which can be used in a further process.

For the distillation process, Zhang et al. (2010) states a heat requirement of 45 $^{kJ}/_{mol\ CH_3OH}$ for an advanced five-column process and 68 $^{kJ}/_{mol\ CH_3OH}$ for a less expensive four-column process. For further calculation, we assume that the synthesis reaction heat covers this demand. If the synthesis gas contains CO instead of CO_2, the excess heat increases, which allows to not only cover the demand for the distillation, but use approximately 35 $^{kJ}/_{mol\ CH_3OH}$ for a further process.

6.2. Storage and transportation

Since Methanol is liquid at standard conditions it is well suited for storage and transportation. An energy consumption of 0.2% - 0.4% per 100 km for the transportation by trucks or railway tank wagons is reported in Wernicke et al. (2014), which is negligible for further calculations. Similar to the transportation, the energy consumption for methanol storage is assumed to be insignificant and is not considered within this analysis.

6.3. Well-to-miles analysis

In Table 9, well-to-miles results for a reference and a future scenario are presented. While the reference scenario considers PEM or alkaline electrolysis with a mean efficiency of 60%, the future scenario directly produces synthesis gas by high temperature co-electrolysis and uses the thermal energy of the exothermic methanol synthesis.

The resulting well-to-miles analysis of methanol is similar to the one of methane, with small differences. While methane needs some energy for storage and transportation, the consumption of methanol storage and transportation can be neglected. However, the methanol synthesis process is more complex and therefore has a higher energy demand. Since this is the dominating difference, the overall energy consumption is slightly higher for methanol.

A total of 4.4 MJ of electric energy is needed to drive a distance of 1 km with synthetic methanol. Approximately 90% of this energy is used for the electrolysis and 10% is needed for CO_2 capturing and the methanol synthesis process. As for all other fuels

Table 9
Synthetic methanol well-to-miles analysis for a reference and a near future scenario, depending on the source of carbon dioxide [biogas, flue gas, seawater, air].

	Reference scenario	Future scenario
Electrolysis	PEM/Alkaline 1210 kJ/mol CH_3OH 60%	SOEC co-electrolysis 991 kJ/mol CH_3OH 77%
CO_2 Separation	for biogas, flue gas, seawater and air: [90, 175, 242, 350] kJ/mol CH_3OH	
CH_3OH Synthesis	Heat unused 40 kJ/mol CH_3OH	Heat → SOEC 40 kJ/mol CH_3OH
Well-to-tank Efficiency	[44, 42, 40, 37]%	[53, 49, 47, 43]%
Well-to-miles Hybrid car	[11.8, 11.1, 10.6, 9.9]% [3.7, 4.0, 4.2, 4.5] MJ/km	[14.1, 13.1, 12.4, 11.5]% [3.1, 3.4, 3.5, 3.8] MJ/km
Well-to-miles Conv. Car	[9.4, 8.8, 8.4, 7.9]% [4.4, 4.7, 4.9, 5.2] MJ/km	[11.2, 10.5, 9.9, 9.1]% [3.7, 3.9, 4.2, 4.5] MJ/km

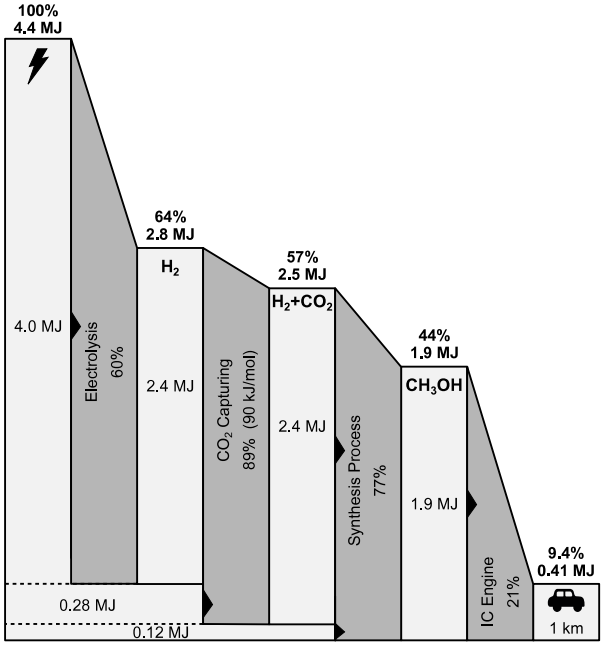

Fig. 5. Well-to-wheels reference scenario for methanol, used in a conventional IC engine vehicle. CO_2 is captured out of biogas.

discussed so far, the electrolysis and the vehicle propulsion system have the highest energy losses. An exchange of the conventional vehicle with a hybrid version would decrease the overall energy demand by 16%. In near future, high-temperature co-electrolysis which reuses excess energy of the synthesis process could further reduce the total energy consumption by another 16%.

For the reference case, Fig. 5 illustrates the well-to-miles analysis for a conventional vehicle and biogas a s a CO_2 source. For this case, a total of 4.4 MJ of electric energy are needed to drive one kilometer.

7. Dimethyl ether

Due to a high cetane number, dimethyl ether (DME) can be used as a renewable fuel in compression–ignition engines.

Dimethyl ether is produced mainly by the dehydration of methanol, as shown in (28). Nowadays, the production of methanol and DME are carried out in separate process steps. However, these two steps can be combined to a single step in order to generate DME from synthesis gas directly. Such combined production plants are topic of ongoing research (Azizi et al., 2014).

$$\begin{aligned} CO_2 + 3H_2 &\longleftrightarrow CH_3OH + H_2O \quad -50\ \text{kJ/mol} \\ 2CH_3OH &\longleftrightarrow CH_3OCH_3 + H_2O \quad -23\ \text{kJ/mol} \end{aligned} \tag{28}$$

For the synthesis of one mole DME, six moles hydrogen are used (28). A comparison of lower heating values shows that 91% of the energy stored in hydrogen can be found in DME after the conversion process. Since the overall reaction is exothermic, no additional energy is needed in theory, which is why the stated value corresponds to the theoretical maximum efficiency.

By considering the electrolysis process, the theoretical maximum electricity to DME efficiency is equal to 77%. If the thermal energy of the overall reaction (123 kJ/mol CH_3OCH_3) is reused in the electrolysis process, the overall efficiency would increase to 83%. An additional increase to 88% can be reached by co-electrolysis.[3]

7.1. Synthesis

According to Fleisch and Sills (2004), DME and methanol production costs are very similar because the additional conversion from methanol to DME is a high yield and low cost step. Although costs do not necessarily correlate with the energy consumption, we assume that the integration of a second reactor between methanol synthesis reactor and purification process operating at similar conditions does not increase the electric energy consumption. Therefore the process needs 80 kJ/mol CH_3OCH_3 of electric energy for compressor work and 110 kJ/mol CH_3OCH_3 or 7% of the synthesis gas cannot be converted to DME, but is used in a burner to produce thermal energy.

If the synthesis gas contains CO instead of CO_2, the methanol synthesis produces 70 kJ/mol CH_3OCH_3 of thermal energy which can be used in another process. In addition we assume that the exothermic methanol-to-DME reaction provides 20 kJ/mol CH_3OCH_3 for further use.

7.2. Storage and transportation

DME is in gaseous state at standard conditions and therefore has to be stored in pressure tanks (vapor pressure at 20 °C: 5.1 bar). According to Arcoumanis et al. (2008), DME fueled vehicles need to have a tank pressure of 12–30 bar to assure that DME is in a liquid state at all time. The energy needed for the compression as well as for the distribution is assumed to be lower than 1% of the stored energy (H_l) and therefore negligible.

7.3. Well-to-miles analysis

Results of the well-to-miles analysis for the reference and the future scenario are listed in Table 10. For the reference scenario with a conventional power-train and biogas as a CO_2 source, the well-to-miles analysis is illustrated in Fig. 6.

Again, the analysis is similar to the one of methane and methanol. The more efficient vehicle power train and a lower energy consumption for storage and transport lead to a slightly improved overall energy consumption compared to methane.

With a total of 4.2 MJ of electric energy, a vehicle fueled with synthetic DME reaches a distance of 1 km. About 10% of this energy is needed for CO_2 capturing and the synthesis process, the rest is used for the electrolysis.

[3] For this calculation, the energy for the CO_2 separation was neglected.

Table 10
Synthetic DME well-to-miles analysis for a reference and a near future scenario, depending on the source of carbon dioxide [biogas, flue gas, seawater, air].

	Reference scenario	Future scenario
Electrolysis	PEM/Alkaline 2420 $^{kJ}/_{mol\ CH_3OCH_3}$ 60%	SOEC co-electrolysis 1960 $^{kJ}/_{mol\ CH_3OCH_3}$ 78%
CO_2 Separation	for biogas , flue gas, seawater and air: [90, 175, 242, 350] $^{kJ}/_{mol\ CH_3OCH_3}$	
CH_3OCH_3 Synthesis	Heat unused 80 $^{kJel}/_{mol\ CH_3OH}$	Heat → SOEC 80 $^{kJel}/_{mol\ CH_3OCH3}$
Well-to-tank Efficiency	[46, 43, 41, 38]%	[54, 51, 48, 45]%
Well-to-miles Hybrid car	[12.8, 12.1, 11.5, 10.7]% [3.4, 3.7, 3.8, 4.1] $^{MJ}/_{km}$	[15.5, 14.4, 13.6, 12.5]% [2.8, 3.1, 3.2, 3.5] $^{MJ}/_{km}$
Well-to-miles Conv. Car	[9.9, 9.3, 8.9, 8.3]% [4.2, 4.4, 4.6, 5.0] $^{MJ}/_{km}$	[12.0, 11.1, 10.5, 9.7]% [3.5, 3.7, 3.9, 4.3] $^{MJ}/_{km}$

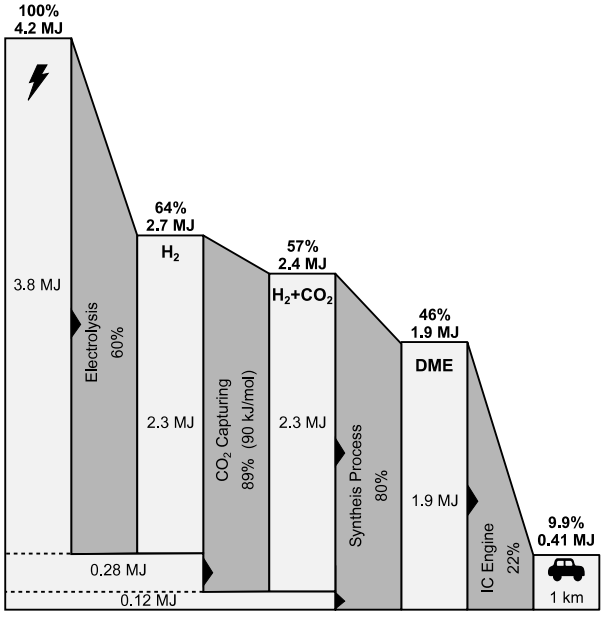

Fig. 6. Well-to-wheels reference scenario for DME, used in a conventional IC engine vehicle. CO_2 is captured out of biogas.

The use of a hybrid vehicle instead of a conventional vehicle improves the overall energy consumption by 19%. Looking at a near-future scenario in which high-temperature co-electrolysis with the reuse of synthesis excess energy is applied, a further improvement of 17% is achieved.

8. Fischer–Tropsch fuels

In 1925, Franz Fischer and Hans Tropsch developed a method for coal liquefaction. After the gasification of coal to synthesis gas, it is converted to hydrocarbons of variable carbon number in a stepwise polymerization reaction, called Fischer–Tropsch process (Yang et al., 2014). Its outcome can be compared to crude oil and is further refined into various fuels as for example gasoline or Diesel.

Eq. (30) states the Fischer–Tropsch reaction, as given in Verdegaal et al. (2015). CO_2 has to be transformed to CO first by the reverse water-gas shift reaction, stated in (29).

$$H_2 + CO_2 \longleftrightarrow CO + H_2O \quad + 41\ ^{kJ}/_{mol} \tag{29}$$

$$CO + 2H_2 \longleftrightarrow -CH_2- + H_2O \quad - 157\ ^{kJ}/_{mol} \tag{30}$$

The products of the Fischer–Tropsch (FT) process consist of light hydrocarbons (methane, ethane, propane butane), naphtha (C_5H_{12} to $C_{12}H_{26}$), kerosene–Diesel fuel ($C_{13}H_{28}$ to $C_{22}H_{46}$), low-molecular-weight wax ($C_{23}H_{48}$ to $C_{32}H_{66}$) and high-molecular-weight wax (> $C_{33}H_{68}$). The chain length distribution of the product depends on the catalyst characteristics, the reaction pressure and temperature, the synthesis gas H_2/CO ratio and further process properties. How these factors influence the FT process is not entirely understood and topic of ongoing research (Lee et al., 2014).

$$CO_2 + 3H_2 \longleftrightarrow -CH_2- + 2H_2O \quad - 116\ ^{kJ}/_{mol} \tag{31}$$

The overall reaction stated in (31) shows that three mol of hydrogen are used for the production of one mol of CH_2 chain links, which have an upper heating value of approximately 610 $^{kJ}/_{mol}$ (Verdegaal et al., 2015). With the enthalpy of water evaporation (44 $^{kJ}/_{mol}$), the lower heating value of one CH_2 chain link can be estimated to 566 $^{kJ}/_{mol}$. Therefore, the theoretical maximum efficiency of the FT process equals to 78%. The theoretical maximum efficiency including the electrolysis process is equal to 66%, but can be increased to 76% if the waste heat of the FT synthesis is reused in the high-temperature electrolysis process. A further increase to 81% is achieved if co-electrolysis is used to directly produce synthesis gas within the electrolysis process.[4]

8.1. Fischer–Tropsch Diesel production

The Fischer–Tropsch synthesis is a complex process that consists of several reactors and its products have to be upgraded in a refinery process in order to reach the desired carbon number.

According to the FT synthesis analysis derived in Becker et al. (2012), the synthesis gas conversion to FT-liquids stated in (30) consumes approximately 50 $^{kJ}/_{mol\ -CH_2-}$ of electric energy (compression of synthesis gas to 40 bar) and 30 $^{kJ}/_{mol\ -CH_2-}$ (distillation, upgrading processes).

The percentage of crude FT synthesis products that can be upgraded to Diesel strongly depends on the carbon number distribution in the FT product, as well as on the refinery process. As stated in van Vliet et al. (2009), about 85% of the crude oil can be refined to synthetic Diesel. The remaining products (85 $^{kJ}/_{mol\ -CH_2-}$) are used in a burner to provide heat for upgrading, distillation or the reverse water-gas shift reaction. Combined with FT synthesis excess heat, there is enough thermal energy available to cover the total Diesel production heat demand.

8.2. Storage, transportation

As for the other liquid fuels, the energy consumption of storage and distribution is very low and therefore negligible in the context of this study. A further advantage of synthetic Diesel is that it can be blended with conventional Diesel without any changes in the existing infrastructure (de Klerk, 2011), which further simplifies storage and transportation.

8.3. Well-to-miles analysis

Results of the well-to-miles analysis for the reference and the future scenario are listed in Table 11. For the reference scenario with a conventional power-train and biogas as a CO_2 source, the well-to-miles analysis is illustrated in Fig. 7.

[4] Note that the Fischer–Tropsch products vary from application to application and therefore, the given values state estimates only. Also, the energy for the CO_2 separation was neglected in these theoretical estimates.

Table 11
Synthetic Diesel well-to-miles analysis for a reference and a near future scenario, depending on the source of carbon dioxide [biogas, flue gas, seawater, air].

	Reference scenario	Future scenario
Electrolysis	PEM/Alkaline 1210 $^{kJ}/_{mol\ -CH_2-}$ 60%	SOEC co-electrolysis 895 $^{kJ}/_{mol\ -CH_2-}$ 86%
CO_2 Separation	for biogas , flue gas, seawater and air: [90, 175, 242, 350] $^{kJ}/_{mol\ -CH_2-}$	
$-CH_2-$ Synthesis	Heat → upgrading 50 $^{kJ}/_{mol\ -CH_2-}$	Heat → upgrading & SOEC 50 $^{kJ}/_{mol\ -CH_2-}$
FT Diesel Upgrading	85% of FT synthesis product converted to FT Diesel	
Well-to-tank Efficiency	[36, 34, 32, 30]%	[46, 43, 41, 37]%
Well-to-miles Hybrid car	[10.0, 9.4, 9.0, 8.4]% [4.4, 4.7, 4.9, 5.3] $^{MJ}/_{km}$	[13.0, 12.0, 11.3, 10.4]% [3.4, 3.7, 3.9, 4.2] $^{MJ}/_{km}$
Well-to-miles Conv. Car	[7.7, 7.2, 6.9, 6.5]% [5.4, 5.7, 6.0, 6.4] $^{MJ}/_{km}$	[10.0, 9.3, 8.8, 8.0]% [4.1, 4.4, 4.7, 5.1] $^{MJ}/_{km}$

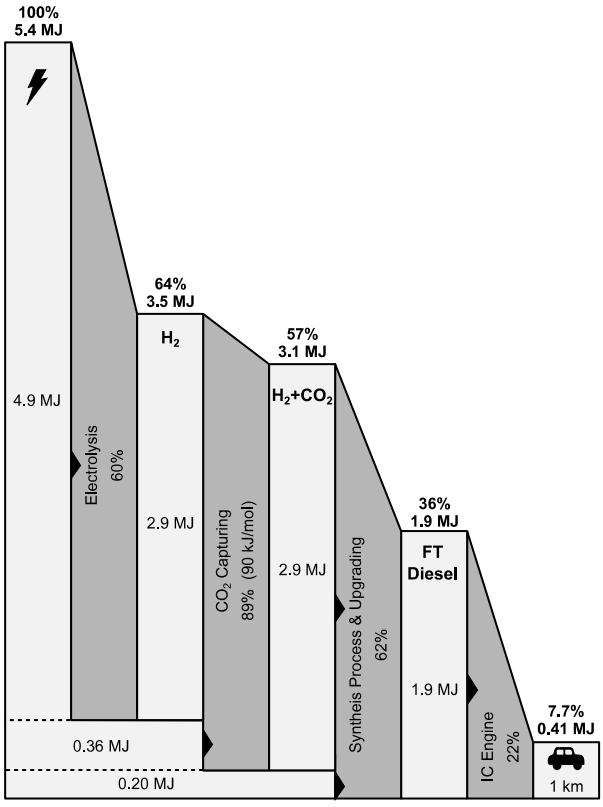

Fig. 7. Well-to-wheels reference scenario for FT-Diesel, used in a conventional IC engine vehicle. CO_2 is captured during the biogas purification.

A total of 5.4 MJ are necessary to drive a distance of 1 km with a vehicle fueled with FT-Diesel. About 10% of the initial energy are needed for the CO_2 separation and the rest of the electricity is used for the electrolysis process. An overall energy reduction of nearly 19% is possible if a hybrid vehicle is used instead of a conventional vehicle. In near future, a further energy reduction of approximately 24% is possible.

9. Synthetic fuel comparison

With the results derived within the last sections, a well-to-miles energy comparison for the five different fuels is presented. In a second step, this comparison is used together with other criteria to derive a simple decision matrix for the power-train technology of various mobile applications.

9.1. Energy consumption comparison of synthetic fuels

A summary of the well-to-miles analysis with biogas as a carbon source for the five investigated fuels is presented in Fig. 8. The mechanical energy at the vehicle wheels, the chemical energy in the vehicle tank and the electric energy for production, storage and distribution are illustrated for conventional as well as hybrid vehicles. The electric energy consumption of the future scenario is marked with gray lines. The mechanical as well as the chemical energy in the vehicle tank do not change for the future scenario. For comparison, the analysis of an electric vehicle, derived in Section 2 is included too.

The analysis of the five investigated fuels clearly shows that the direct use of hydrogen in a fuel cell hybrid vehicle has the lowest energy consumption. Storage and distribution consume considerably more energy for hydrogen compared to other fuels, however, these losses are overcompensated with the efficient fuel cell propulsion system. Vehicles with power-trains based on internal combustion engines have an increased consumption by 9% to 31%, depending on fuel type and hybridization. Further, no carbon capturing or synthesis processes are needed if hydrogen is used as a fuel directly.

Methane, methanol, and DME perform similarly. A conventional vehicle fueled with one of these fuels increases the consumption by approximately 60%, a hybrid vehicle by 30% compared to a fuel cell car. A closer look reveals that even though DME is produced by methanol dehydration in an additional process, the overall energy consumption is slightly lower than for methanol due to advantageous combustion characteristics.

Mainly because the FT Diesel production requires an additional refining process, the well-to-miles analysis reaches the highest energy consumption for this fuel. Compared to a fuel cell vehicle, the initial electric energy doubles. Compared to methane, methanol or DME, the consumption increases by approximately 25%. The future scenario improves the fuel production process due to an increased electrolysis efficiency, the direct reduction of CO_2 to CO with high temperature co-electrolysis and the recycling of thermal energy. For hydrogen, the advanced electrolysis has the potential of a 10% reduction, while for the carbon fuels the potential is approximately 20% compared to the reference scenario. A further reduction of 5% for hydrogen is realized by pipeline transportation, compared to the road transportation by tube trailers.

For vehicles with an internal combustion engine, hybridization (charge sustaining operation) offers a reduction potential by approximately 20%. A further improvement in energy consumption can be derived by plug-in hybrid electric vehicles (PHEV), which use both electricity and synthetic fuel as an energy source. Such vehicles can reach any energy consumption between an electric vehicle and a charge sustaining hybrid vehicle, depending on the electricity-to-synthetic-fuel ratio they are operated with.

The direct use of electricity in an electric vehicle without any energy conversion in between of course leads to the lowest energy consumption. Even for the future scenario with charge sustaining hybridization, fuel cell vehicles consume approximately 3 times more energy. Cars fueled with methane, methanol or DME need about 4 times more energy and a vehicle fueled with FT Diesel has a 4.5 times higher energy consumption.

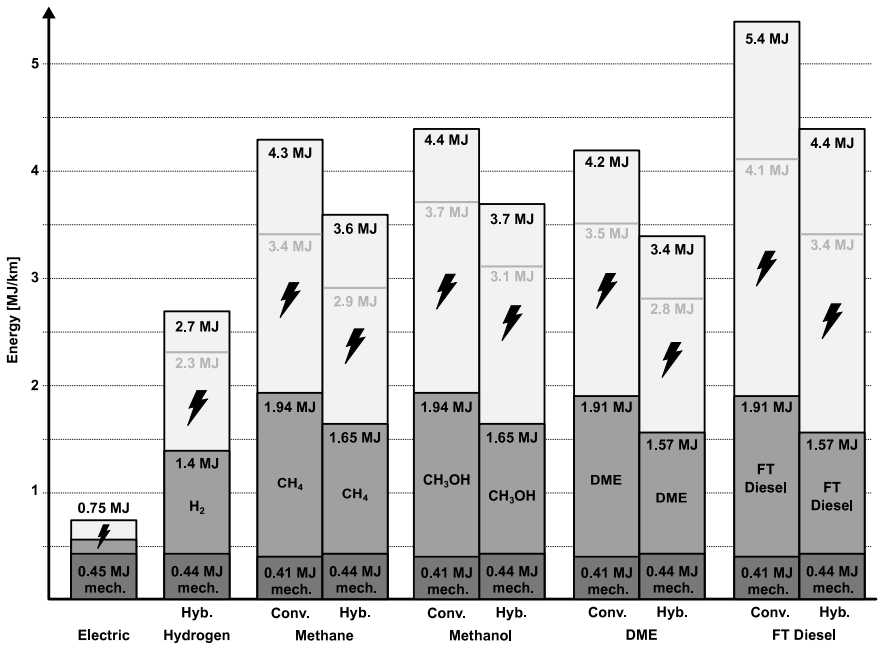

Fig. 8. Well-to-miles analysis results for the five investigated synthetic fuels, produced with CO_2 from a biogas purification process. In addition, an electric vehicle is included for comparison. For the electricity consumption, values in black illustrate the reference scenario and values in gray refer to the future scenario.

9.2. Vehicle choice for mobile applications

Various mobile applications have various performance requirements. We consider the energy consumption as a basic performance criteria for all mobile applications and introduce three further criteria, which apply for certain applications only. These are the need for on-road refueling, the refueling time and the necessity for the application to be lightweight.

For all the investigated power-train technologies, the qualification to fulfill these criteria is evaluated on a qualitative level.[5]

For very lightweight applications, conventional internal combustion propulsion systems offer the highest energy density. For all the other applications, the choice of powertrain depends on the necessity of fast and on-road refueling. If a high density of filling stations is an absolute necessity and refueling has to be fast, a synthetic Diesel hybrid vehicle is a suitable choice. However, this application has a 4.5 times higher energy consumption compared to an electric vehicle. If a medium density of filling stations is sufficient, a synthetic methane hybrid vehicle with a 4 times higher energy consumption is proposed.

Applications without the need of on-road refueling are independent of existing filling station infrastructure and can therefore be further optimized for energy consumption. For applications with the need of fast refueling, a hydrogen PHEV is proposed. Compared to the methane PHEV used for on-road refueling, this power-train reduces the consumption from 4 to 3 times the energy of an electric car.

If fast refueling is not always necessary but needs to be possible, the use of a plug-in hybrid electric vehicle instead of a classic charge-sustaining hybrid vehicle offers a further energy consumption reduction. If refueled with electricity only, a PHEV has the same consumption as an electric vehicle. If refueled fast with synthetic fuel, it reaches the consumption of its according charge-sustaining hybrid vehicle.

For all non-lightweight applications without the need of fast refueling, electric vehicles are the best fit.

[5] The on-road refueling criteria represents the existing filling station density in central Europe. The lightweight criteria is evaluated as a combination of propulsion system weight and fuel density. The energy consumption criteria refers to the near-future scenario derived in this study.

10. Conclusion

A well-to-miles analysis for the five different synthetic fuels hydrogen, me-thane, methanol, dimethyl-ether and Fischer–Tropsch Diesel is derived within this study. Starting with renewable electricity, water and carbon dioxide captured from various sources, the fuel production process steps (including storage and distribution) are described and characterized by their energy consumption based on a literature study, which is complemented with own research data and data from commercially available technologies. For the tank-to-miles analysis, a power-train model based on the Willans approach is derived and identified for each synthetic fuel with chassis dynanometer data of different EURO-6b passenger car types. Combined with a dynamic vehicle chassis model (Guzzella and Sciarretta, 2013), the power-train model is used to simulate a WLTC class 3 cycle in order to derive the mean fuel energy demand per kilometer.

An energy consumption comparison of the five fuels shows that fuel cell vehicles have a clear advantage over vehicles powered with methane, methanol or DME. Fischer–Tropsch fuels have the highest energy demand due to a lower synthesis process selectivity. High-temperature co-electrolysis has the potential to improve the well-to-miles energy consumption of carbon-based fuels by approximately 20%. Compared to conventional vehicles, charge-sustaining hybrid electric vehicles reduce the consumption by another 20%. The use of plug-in electric vehicles allows any consumption between the electric vehicle and the according charge-sustaining hybrid vehicle, depending on the ratio of synthetic fuel and electricity they are operated with.

Acknowledgments

The measurement series used for the identification of the vehicle models was conducted at Empa Dübendorf (Switzerland) within the emission inventory project on behalf of the Swiss federal office for the environment (FOEN).

Appendix

A description of all symbols and abbreviations can be found in the Tables A.12 and A.13.

Table A.12
Description and unit definition of all symbols.

Symbol	Description	Unit
γ	Ratio of specific heats	–
ΔG_R	Specific Gibbs free energy enthalpy	$^{kJ}/_{mol}$
ΔH_R	Specific reaction enthalpy	$^{kJ}/_{mol}$
ΔS_R	Specific reaction entropy	$^{kJ}/_{mol\ K}$
η_{prod}	Efficiency for a process in the fuel production	–
η_{TtW}	Wheel power dependent power-train efficiency	–
$\eta_{TtW,mean}$	Mean power-train efficiency for a test drive cycle	–
η_{use}	Efficiency for a process in the fuel consumption	–
ρ_{air}	Density of air	$^{kg}/_{m^3}$
σ	Standard deviation	%
A_f	Frontal vehicle area	m^3
$c_{1,pos}$, $c_{1,neg}$	Willans power-train model parameter	–
$c_{0,pos}$, $c_{0,neg}$	Willans power-train model parameter	kW
c_d	aerodynamic drag coefficient	–
c_r	rolling friction coefficient	–
E_{adi}	Specific energy for an adiabatic gas compression	$^{kJ}/_{mol}$
$E_{chem,norm}$	Mean fuel energy (H_l) needed for a 1 km drive	$^{MJ}/_{km}$
E_{comp}	Specific energy for a gas compression	$^{kJ}/_{mol}$
E_{isoth}	Specific energy for an isothermal gas compression	$^{kJ}/_{mol}$
E_{prod}	Energy content of the produced fuel	kJ
E_{wheels}	Mechanical energy acting at the vehicle wheels	kJ
$E_{wheels,norm}$	Mean mechanical energy needed for a 1 km drive	$^{kJ}/_{km}$
g	gravitational acceleration	$^{m}/_{s^2}$
H_l	lower heating value of a fuel	$^{kJ}/_{mol}$
H_u	upper heating value of a fuel	$^{kJ}/_{mol}$
m_{fuel}	fuel amount	mol
m_{car}	car mass	kg
p_0	gas pressure before compression	Pa
p_1	gas pressure after compression	Pa
P_{acc}	Vehicle acceleration power	kW
P_{aero}	Vehicle power lost in air friction	kW
P_{chem}	Fuel power (H_l)	kW
P_{roll}	Vehicle power lost in rolling friction	kW
p_{store}	fuel storage tank pressure	bar
p_{tank}	vehicle tank pressure	bar
P_{wheels}	Mechanical power at the vehicle wheels	kW
t	time	s
R^2	Mean coefficient of determination	%
T	Reaction temperature	°K
v	vehicle speed	$^{m}/_{s}$
V_0	gas volume before compression	m^3
V_1	gas volume after compression	m^3

Table A.13
Abbreviations.

WLTC	Worldwide harmonized Light vehicles Test Cycle
CNG	Compressed Natural Gas
Conv.	Conventional
DME	Di-Methyl Ether
FC	Fuel Cell
FOEN	Swiss Federal Office for Environment
FT	Fischer–Tropsch
HEV	Hybrid Electric Vehicle
Hyb.	Hybrid
PEM	Proton Exchange Membrane
PHEV	Plugin Hybrid Electric Vehicle
SOEC	Solid Oxide Electrolyte Cell
TtM	Tank-to-Miles
TtW	Tank-to-Wheels
WtM	Well-to-miles
WtM	Wheels-to-Miles
WtW	Well-to-Wheels

References

Arcoumanis, C., Bae, C., Crookes, R., Kinoshita, E., 2008. The potential of di-methyl ether (DME) as an alternative fuel for compression-ignition engines: A review. Fuel 87 (7), 1014–1030.

Aziz, M.A.A., Jalil, A.A., Triwahyono, S., Ahmad, A., 2015. CO 2 methanation over heterogeneous catalysts: Recent progress and future prospects. Green Chem..

Azizi, Z., Rezaeimanesh, M., Tohidian, T., Rahimpour, M.R., 2014. Dimethyl ether: A review of technologies and production challenges. Chem. Eng. Process. : Process Intensif. 82 (150).

Bach, C., Soltic, P., 2011. CO2 Reduction and cost efficiency potential of natural gas hybrid passenger cars. SAE Int. J. Engines 4 (2), 2395.

Becker, W., Braun, R., Penev, M., Melaina, M., 2012. Production of Fischertropsch liquid fuels from high temperature solid oxide co-electrolysis units. Energy 47 (1), 99–115.

Bossel, U., 2006. Does a hydrogen economy make sense? Proc. IEEE 94 (10), 1826–1837.

Brynolf, S., Taljegard, M., Grahn, M., Hansson, J., 2018. Electrofuels for the transport sector: A review of production costs. Renew. Sustain. Energy Rev. 81, 1887–1905.

Cabalzar, U., Stadelmann, P., 2017. 70 MPa H2 Tankstellen - Aufbau und Betrieb der ersten Wasserstoff- Tankstellen in der Schweiz mit einem Nenndruck von 70 MPa. Tech. rep., Bundesamt für Energie (BFE) und EMPA Dübendorf.

Creutzig, F., Jochem, P., Edelenbosch, O.Y., Mattauch, L., Vuuren, D. P. v., McCollum, D., Minx, J., 2015. Transport: A roadblock to climate change mitigation? Science 350 (6263), 911–912.

Desideri, U., Paolucci, A., 1999. Performance modelling of a carbon dioxide removal system for power plants. Energy Convers. Manage. 40 (18), 1899–1915.

Eisaman, M.D., Parajuly, K., Tuganov, A., Eldershaw, C., Chang, N., Littau, K.A., 2012. CO 2 extraction from seawater using bipolar membrane electrodialysis. Energy Environ. Sci. 5 (6), 7346–7352.

ETOGAS GmbH, 2015. Power-to-Gas: Energiewende in allen energiesektoren. In: Technology Briefing: Power-to-Gas in der Mobilität. EMPA Dübendorf, pp. 1–19.

Evans, Simon, 2017. The Swiss company hoping to capture 1% of global CO2 emissions by 2025. https://www.carbonbrief.org/.

Fasihi, M., Bogdanov, D., Breyer, C., 2016. Techno-economic assessment of power-to-liquids (ptl) fuels production and global trading based on hybrid pv-wind power plants. Energy Procedia 99, 243–268, 10th International Renewable Energy Storage Conference, IRES 2016, pp. 15–17 Düsseldorf, Germany. http://www.sciencedirect.com/science/article/pii/S1876610216310761.

Fleisch, T.H., Sills, R.A., 2004. Large-scale gas conversion through oxygenates: Beyond GTL-FT. In: Xu, X.B., Yide (Eds.), Natural Gas Conversion VII Proceedings of the 7th Natural Gas Conversion Symposium. Elsevier, pp. 31–36.

Fu, Q., Mabilat, C., Zahid, M., Brisse, A., Gautier, L., 2010. Syngas production via high-temperature steam/CO 2 co-electrolysis: An economic assessment. Energy Environ. Sci. 3 (10), 1382–1397.

Gallandat, N., Romanowicz, K., Züttel, A., 2017. An analytical model for the electrolyser performance derived from materials parameters. J. Power Energy Eng. 05 (10), 34.

Gebald, C., 2014. Development of amine-functionalized adsorbent for carbon dioxide capture from atmospheric air. Ph.D. Thesis. ETH-Zürich.

Guzzella, L., Sciarretta, A., 2013. Vehicle propulsion systems. pp. 1–419.

Jadhav, S.G., Vaidya, P.D., Bhanage, B.M., Joshi, J.B., 2014. Catalytic carbon dioxide hydrogenation to methanol: A review of recent studies. Chem. Eng. Res. Des. 92 (11), 2557–2567.

de Klerk, A., 2011. Fischer–Tropsch refining. In: DE KLERK:FISCHER-TROPSCH O-BK. Wiley-VCH Verlag GmbH & Co. KGaA, Weinheim, Germany.

Larsson, M., Grnkvist, S., Alvfors, P., 2015. Synthetic fuels from electricity for the swedish transport sector: Comparison of well to wheel energy efficiencies and costs. Energy Procedia 75, pp. 1875–1880, clean, Efficient and Affordable Energy for a Sustainable Future: The 7th International Conference on Applied Energy, ICAE2015.

Lee, S., Speight, J.G., Loyalka, S.K., 2014. Handbook of Alternative Fuel Technologies, second ed. CRC Press.

Luo, X., Wang, J., Dooner, M., Clarke, J., 2015. Overview of current development in electrical energy storage technologies and the application potential in power system operation. Appl. Energy 137, 511–536, http://www.sciencedirect.com/science/article/pii/S0306261914010290.

Müller, B., Müller, K., Teichmann, D., Arlt, W., 2011. Energiespeicherung mittels Methan und energietragenden Stoffen – ein thermodynamischer Vergleich. Chem. Ing. Tech. 83 (11), 2002–2013.

Ott, T., Zurbriggen, F., Onder, C., Guzzella, L., 2013. Cycle-averaged efficiency of hybrid electric vehicles. Proceedings of the institution of mechanical engineers. Part D: J. Automob. Eng. 227 (1), 78–86.

Reiche, D., Bechberger, M., 2004. Policy differences in the promotion of renewable energies in the eu member states. Energy Policy 32 (7), 843–849.

Reiter, G., Lindorfer, J., 2015. Global warming potential of hydrogen and methane production from renewable electricity via power-to-gas technology. Int. J. Life Cycle Assess. 1–13.

Semelsberger, T.A., Borup, R.L., Greene, H.L., 2006. Dimethyl ether (DME) as an alternative fuel. J. Power Sources 156 (2), 497–511.

Sunfire GmbH, 2017. Sunfire steam electrolyser. http://www.sunfire.de.

The Linde Group, 2013. Linde setzt neue Massstaebe beim Wasserstofftransport. http://www.the-linde-group.com.

The Linde Group, 2017. Hydrogen technologies - The ionic compressor 90MPa - IC90. http://www.the-linde-group.com.

Töpler, J., Lehmann, J., 2014. Wasserstoff und Brennstoffzelle. Springer, Berlin, Heidelberg.

Ursua, A., Gandia, L.M., Sanchis, P., 2012. Hydrogen production from water electrolysis: Current status and future trends. Proc. IEEE 100 (2), 410–426.

Van-Dal, verton Simes, Bouallou, C., 2013. Design and simulation of a methanol production plant from CO2 hydrogenation. J. Cleaner Prod. 57, 38–45, http://www.sciencedirect.com/science/article/pii/S0959652613003892.

Verbeek, R., Van der Weide, J., 1997. Global assessment of dimethyl-ether: Comparison with other fuels. In: International Spring Fuels & Lubricants Meeting & Exposition. SAE International.

Verdegaal, W.M., Becker, S., Olshausen, C.v., 2015. Power-to-Liquids: Synthetisches Rohöl aus CO2Wasser und Sonne. Chem. Ing. Tech. n/a–n/a.

van Vliet, O., Faaij, A., Turkenburg, W., 2009. Fischertropsch diesel production in a well-to-wheel perspective: A carbon, energy flow and cost analysis. 50, pp. 855–876.

Weitemeyer, S., Kleinhans, D., Vogt, T., Agert, C., 2015. Integration of renewable energy sources in future power systems: The role of storage. Renew. Energy 75, 14–20.

Wendt, H., Vogel, G.H., 2014. Die Bedeutung der Wasserelektrolyse in Zeiten der Energiewende. Chem. Ing. Tech. 86 (1–2), 144–148.

Wernicke, H.-J., Plass, L., Schmidt, F., 2014. Methanol generation. In: Bertau, M., Offermanns, H., Plass, L., Schmidt, F., Wernicke, H.-J. (Eds.), Methanol: The Basic Chemical and Energy Feedstock of the Future. Springer, Berlin, Heidelberg, pp. 51–301–301.

Willauer, H.D., DiMascio, F., Hardy, D.R., Williams, F.W., 2014. Feasibility of CO2 extraction from seawater and simultaneous hydrogen gas generation using a novel and robust electrolytic cation exchange module based on continuous electrodeionization technology. Ind. Eng. Chem. Res. 53 (31), 12192–12200.

Yang, J., Ma, W., Chen, D., Holmen, A., Davis, B.H., 2014. Fischer–Tropsch synthesis: A review of the effect of CO conversion on methane selectivity. Appl. Catalysis A: General 470 IS, 250–260.

Zeman, F., 2007. Energy and material balance of CO2 capture from ambient air. Environ. Sci. Technol. 41 (21), 7558–7563.

Zhang, J., Liang, S., Feng, X., 2010. A novel multi-effect methanol distillation process. Chem. Eng. Process. : Process Intensif. 49 (10), 1031–1037.